Advances in Applied Mathematics and Mechanics
Adv. Appl. Math. Mech., Vol. 7, No. 1, pp. 116-134

DOI: 10.4208/aamm.2013.m143
February 2015

Thermodynamical Bending of FGM Sandwich Plates Resting on Pasternak's Elastic Foundations

Mohammed Sobhy[1,3] and Ashraf M. Zenkour[2,3,*]

[1] *Department of Mathematics, Faculty of Science, King Faisal University, P.O. Box 400, Hufof 31982, Saudi Arabia*
[2] *Department of Mathematics, Faculty of Science, King Abdulaziz University, P.O. Box 80203, Jeddah 21589, Saudi Arabia*
[3] *Department of Mathematics, Faculty of Science, Kafrelsheikh University, Kafrelsheikh 33516, Egypt*

Received 8 March 2013; Accepted (in revised version) 25 April 2014

Abstract. The analysis of thermoelastic deformations of a simply supported functionally graded material (FGM) sandwich plates subjected to a time harmonic sinusoidal temperature field on the top surface and varying through-the-thickness is illustrated in this paper. The FGM sandwich plates are assumed to be made of three layers and resting on Pasternak's elastic foundations. The volume fractions of the constituents of the upper and lower layers and, hence, the effective material properties of them are assumed to vary in the thickness direction only whereas the core layer is still homogeneous. When in-plane sinusoidal variations of the displacements and the temperature that identically satisfy the boundary conditions at the edges, the governing equations of motion are solved analytically by using various shear deformation theories as well as the classical one. The influences of the time parameter, power law index, temperature exponent, top-to-bottom surface temperature ratio, side-to-thickness ratio and the foundation parameters on the dynamic bending are investigated.

AMS subject classifications: 74XX

Key words: FGM sandwich plates, dynamic bending, elastic foundations, thermal load.

1 Introduction

Sandwich structures have high structural efficiency because of their excellent properties such as high ratio of strength-to-weight, good energy and sound absorption capability, and often low production cost. They are mainly used in aerospace, marine and aircraft

*Corresponding author.
Email: zenkour@kau.edu.sa or zenkour@sci.kfs.edu.eg (A. M. Zenkour)

 ©2015 Global Science Press

industry as thin-walled structures but at present the application of these structures has been extended to automobile, petrochemical and other industries. Structural sandwich is basically fabricated from three layers. The two face sheets adhesively bonded to the core. The traditional sandwich structures have some drawbacks. The sudden change in material properties across the interfaces among different materials can result in large interlaminar stresses. To overcome these disadvantages, FGMs composed of two or more phases with different material properties and continuously varying composition distribution have been used as a core layer or face layers. Such materials were introduced to take advantage of the desired material properties of each constituent material without interface problems. Owing to these reasons, a number of research works about the sandwich structures with FGM face layers have been established, in particular to study their elastic [1] and thermo-elastic behavior [2–4]. To investigate the effect of FGM core on performance of sandwich plates, Anderson [5] and Kashtalyan and Menshykova [6] have developed the 3-D elasticity solution for sandwich composites with a FG core subjected to transverse loading.

FGMs are widely used in many engineering applications, for example aerospace, automotive and biomedical applications. Thus, many works on FGM structures have been studied in literature. For example, Reddy [7] has analyzed the static behavior of FG rectangular plates based on his third-order shear deformation plate theory. Reddy and Chen [8] have presented a three-dimensional model for a FG plate subjected to mechanical and thermal loads, both applied at the top of the plate. Vel and Batra [9] have proposed a three-dimensional solution for transient thermal stresses in FG rectangular plates. Also, several investigations on the behavior of the FGM plates, disks and cylinders have been explained in Zenkour [10–14], Zenkour et al. [15] and Zenkour and Sobhy [16, 17].

Structures resting on elastic foundations is often encountered in the analysis of the foundations of buildings, highway and railroad structures, and of geotechnical structures [18]. The simplest and most frequently employed elastic foundation model is that of Winkler [19], which is generally referred to as a one-parametric model. The transverse deformation characteristics of the elastic foundation are defined by means of continuous and closely spaced linear springs providing resistance in direct proportion to the deflection of the plate. The deficiency of Winkler's formulation is the behavioral inconsistency due to the discontinuity of displacements on the boundary of the uniformly loaded surface area [20]. To add the influence of shear effect of the foundation besides the vertical springs, Pasternak [21] had introduced a shear layer such that it is an incompressible vertical element and deforms only by transverse shear force. Many formulations of the equations of dynamic and static equilibrium of structures on Winkler's elastic foundation [22–24] or Pasternak's ones [25–29] are to be encountered in the literature.

Thermal effects could be important when a mechanical system has undergo high or low temperature gradients. Thus, the effect of thermal loading on the displacement and stress fields for FGM plates and shells has been studied by a number of authors. Praveen and Reddy [30] have employed the finite element method to illustrate the response of

FG ceramic-metal plates under thermal load. On the basis of the first-order shear deformation plate theory, the static responses of metal and ceramic FGM plates subject to thermal and mechanical loads have been investigated by Lee et al. [31]. Transient thermoelastic responses of FGMs containing collinear cracks have been studied by Noda and Wang [32]. Vel and Batra [33] have presented an exact solution for thermoelastic deformations of FG thick rectangular plates. Zenkour and Sobhy [34, 35] have derived stability equations of FGM sandwich plates and FGM one resting on elastic foundations under thermal loads based on sinusoidal shear deformation plate theory (SDPT). Shen [36] has studied the nonlinear bending response of FGMs subjected to transverse loads and in a thermal environment.

The dynamic bending behavior of a FG sandwich plates resting on two-parameter elastic foundations and subjected to a through-the-thickness temperature field is investigated. The material properties of the FG layers are assumed to vary continuously through the thickness according to a simple power law distribution of the volume fraction of the constituents. The equations of motion are derived using the SDPT and they contain the thermal effect and the interaction between the plate and the elastic foundations. The results obtained by the SDPT are compared with those obtained by the classical plate theory (CPT), the first-order shear deformation plate theory (FDPT) and the higher-order one (HDPT). Some numerical examples are provided to demonstrate the effects of various parameters on the dynamic bending of the FGM sandwich plates.

2 Mathematical model

Consider a rectangular sandwich plate of length a, width b and thickness h made of functionally graded material. The FGM sandwich plate is supported at four edges defined in the (x, y, z) coordinate system with x- and y-axes located in the middle plane ($z=0$) and its origin placed at the corner of the plate as shown in Fig. 1. It is subjected to a time harmonic sinusoidal temperature field on the top surface and varying through-the-thickness.

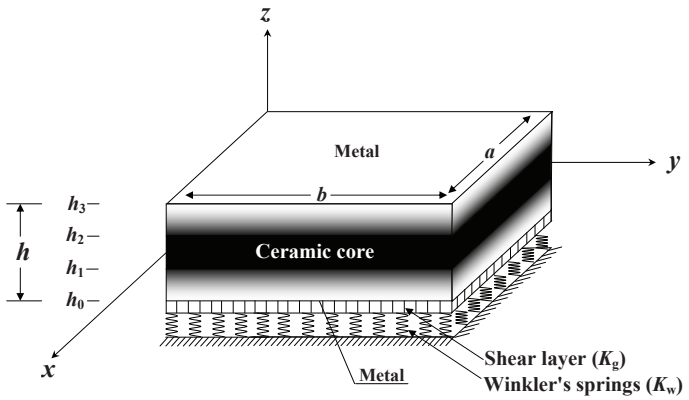

Figure 1: Geometry of the FGM sandwich plate resting on two parameter elastic foundations.

The face layers of the sandwich plate are made of a functionally graded material with material properties varying smoothly in the z (thickness) direction only. Material properties at a point are usually assumed to be given by the rule of mixture [1,2,34]

$$P^{(n)}(z)=P_{\rm m}+(P_{\rm c}-P_{\rm m})V^{(n)}, \tag{2.1}$$

where P represents the elastic coefficients E_1, E_2 and E_3, the stress-temperature modulus ξ and the density ρ. The subscripts m and c refer to metal and ceramic materials. The elastic coefficients and the stress-temperature modulus will be defined later. $V^{(n)}$ is the volume fraction of layer n which is equal to unity in the core (i.e., $V^{(2)}=1$, at $h_1\leq z\leq h_2$) while it follows a simple power law through the thickness of the bottom and top layers that takes the form

$$V^{(1)}=\Big(\frac{z-h_0}{h_1-h_0}\Big)^k, \qquad h_0\leq z\leq h_1, \tag{2.2a}$$

$$V^{(3)}=\Big(\frac{z-h_3}{h_2-h_3}\Big)^k, \qquad h_2\leq z\leq h_3, \tag{2.2b}$$

where k is a parameter which denotes the power law index and takes values greater than or equal to zero. The core is independent of the value of k which is fully ceramic. Note that the value of k equaling to zero represents a homogeneous isotropic ceramic plate and the value of it equaling to infinity represents a metal-ceramic-metal (m-c-m) sandwich plate. The above power law assumption reflects a simple rule of mixtures used to obtain the effective properties of the metal-ceramic sandwich plate (see Fig. 1). Also, note that the volume fraction of the ceramic is high near the interfaces, and that of the metal is high near the bottom and top surfaces.

2.1 Various types of FGM sandwich plates

Fig. 2 shows the through-the-thickness variation of the volume fraction function of the material for $k=1,2,3,5,7$. Note that the core of the symmetric and nonsymmetric plates are fully ceramic while the bottom and the top surfaces of the plate are metal-rich.

2.1.1 The (1-1-1) FGM sandwich plate

As shown in Fig. 2(a), the plate is made of three equal-thickness layers. So, one gets

$$h_1=-\frac{h}{6}, \quad h_2=\frac{h}{6}. \tag{2.3}$$

2.1.2 The (2-1-2) FGM sandwich plate

In this state the core of the plate is half the face thickness (see Fig. 2(b)). Thus,

$$h_1=-\frac{h}{10}, \quad h_2=\frac{h}{10}. \tag{2.4}$$

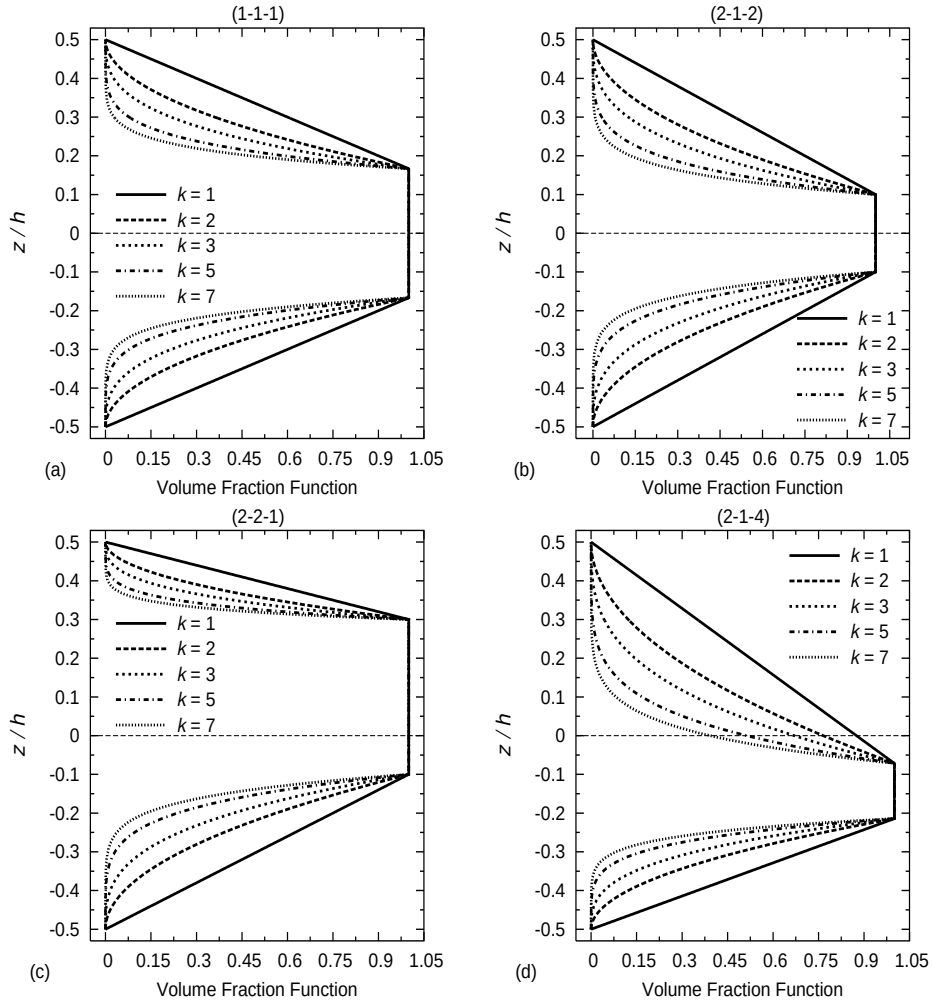

Figure 2: Through-thickness distributions of volume fraction function for various values of the power law index k and various types of FGM sandwich plates: (a) The (1-1-1) FGM sandwich plate, (b) The (2-1-2) FGM sandwich plate, (c) The (2-2-1) FGM sandwich plate, (d) The (2-1-4) FGM sandwich plate.

2.1.3 The (2-2-1) FGM sandwich plate

Here the sandwich plate is nonsymmetric about the mid-plane in which the core thickness equals the lower face thickness while it is twice the upper face thickness (see Fig. 2(c)). Thus, we have

$$h_1=-\frac{h}{10},\quad h_2=\frac{3h}{10}. \tag{2.5}$$

2.1.4 The (2-1-4) FGM sandwich plate

In this case the sandwich plate is also nonsymmetric about the mid-plane such that the core thickness is half the lower face thickness, but it equals one-fourth the upper face thickness (see Fig. 2(d)). Then

$$h_1=-\frac{3h}{14},\quad h_2=-\frac{h}{14}. \tag{2.6}$$

The FGM sandwich plates are considered to be resting on two-parameter elastic foundations. The foundation is assumed to be attached to the plate and separation does not arise. The load-displacement relationship of the foundation is presumed to be

$$R=K_{\rm w}w-K_{\rm p}\nabla^2 w, \tag{2.7a}$$

where w is the plate deflection, R is the force per unit area, $K_{\rm w}$ and $K_{\rm p}$ are the Winkler's and Pasternak's foundation stiffnesses and ∇^2 is the Laplace operator in x and y.

The displacement field, taking into account the shear deformation effect, is presented for FGM sandwich plates as

$$u_x(x,y,z,t)=u-z\partial_x w+g(z)\varphi_x,\quad u_y(x,y,z,t)=v-z\partial_y w+g(z)\varphi_y,\quad u_z(x,y,z,t)=w, \tag{2.8}$$

where u, v, w, φ_x and φ_y are independent of z and the function $g(z)=0$ for the CPT, $g(z)=z$ for the FDPT, $g(z)=z(1-4z^2/3h^2)$ for the HDPT and $g(z)=h\pi^{-1}\sin(\pi z/h)$ for the SDPT. The functions u, v and w give displacements of a point on the mid-surface of the plate and φ_x and φ_y are, respectively, rotations of the transverse normal to the mid-surface about the y- and x-axis.

The strain tensor for infinitesimal deformations is related to the displacements u_j by

$$\varepsilon_j=\partial_j u_j,\quad \gamma_{j\ell}=\partial_j u_\ell+\partial_\ell u_j,\quad j,\ell=x,y,z,\quad j\neq\ell. \tag{2.9}$$

Substitution from Eq. (2.8) into Eq. (2.9) yields the following equations

$$\varepsilon_x=\partial_x u-z\partial_x^2 w+g\partial_x\varphi_x,\quad \varepsilon_y=\partial_y v-z\partial_y^2 w+g\partial_y\varphi_y,\quad \varepsilon_z=0, \tag{2.10a}$$

$$\gamma_{xy}=\partial_x v+\partial_y u-2z\partial_x\partial_y w+g(\partial_x\varphi_y+\partial_y\varphi_x),\quad \gamma_{yz}=g'\varphi_y,\quad \gamma_{xz}=g'\varphi_x, \tag{2.10b}$$

where $g'={\rm d}g/{\rm d}z$.

The stress-strain relations for a linear isotropic elastic plate are given by

$$\sigma_x^{(n)}=E_1^{(n)}\varepsilon_x+E_2^{(n)}\varepsilon_y+\xi^{(n)}T(x,y,z,t),\quad \sigma_y^{(n)}=E_1^{(n)}\varepsilon_y+E_2^{(n)}\varepsilon_x+\xi^{(n)}T(x,y,z,t), \tag{2.11a}$$

$$\tau_{xy}^{(n)}=E_3^{(n)}\gamma_{xy},\quad \tau_{yz}^{(n)}=E_3^{(n)}\gamma_{yz},\quad \tau_{xz}^{(n)}=E_3^{(n)}\gamma_{xz}, \tag{2.11b}$$

where

$$E_1^{(n)}=\frac{E_{(n)}}{1-\nu_{(n)}^2},\quad E_2^{(n)}=\frac{\nu_{(n)}E_{(n)}}{1-\nu_{(n)}^2},\quad E_3^{(n)}=\frac{E_{(n)}}{2(1+\nu_{(n)})},\quad \xi^{(n)}=\frac{E_{(n)}\alpha_{(n)}}{\nu_{(n)}-1}, \tag{2.12}$$

in which $E_{(n)}$, $\nu_{(n)}$ and $\alpha_{(n)}$ are Young's modulus, Poisson's ratio and the coefficient of thermal expansion for the n-th layer, respectively. Note that they are functions of z and they are given according to Eq. (2.1).

3 Equations of motion

The dynamic version of the principle of virtual displacements in the present study yields

$$\int_{-h/2}^{h/2}\int_{\Omega}\Big[\rho_{(n)}\ddot{u}_j\delta u_j+\sigma_{xx}^{(n)}(\varepsilon_{xx}-\alpha_{(n)}T)+\sigma_{yy}^{(n)}(\varepsilon_{yy}-\alpha_{(n)}T)+\sigma_{xy}^{(n)}\gamma_{xy}+\sigma_{yz}^{(n)}\gamma_{yz} +\sigma_{xz}^{(n)}\gamma_{xz}\Big]d\Omega dz+\int_{\Omega}R\delta w d\Omega=0,\quad j=x,y,z. \tag{3.1}$$

The governing equations of motion can be derived by using the above principle of virtual displacements as

$$\partial_x N_x+\partial_y N_{xy}=I_0\ddot{u}-I_1\partial_x\ddot{w}+I_2\ddot{\varphi}_x, \tag{3.2a}$$
$$\partial_x N_{xy}+\partial_y N_y=I_0\ddot{v}-I_1\partial_y\ddot{w}+I_2\ddot{\varphi}_y, \tag{3.2b}$$
$$\partial_x^2 M_x+2\partial_x\partial_y M_{xy}+\partial_y^2 M_y-R=I_0\ddot{w}+I_1\big(\partial_x\ddot{u}+\partial_y\ddot{v}\big)-I_3\big(\partial_x^2\ddot{w}+\partial_y^2\ddot{w}\big) +I_4\big(\partial_x\ddot{\varphi}_x+\partial_y\ddot{\varphi}_y\big), \tag{3.2c}$$
$$\partial_x M_x^s+\partial_y M_{xy}^s-Q_{xz}=I_2\ddot{u}-I_4\partial_x\ddot{w}+I_5\ddot{\varphi}_x, \tag{3.2d}$$
$$\partial_x M_{xy}^s+\partial_y M_y^s-Q_{yz}=I_2\ddot{v}-I_4\partial_y\ddot{w}+I_5\ddot{\varphi}_y, \tag{3.2e}$$

where N_{xx}, N_{yy} and N_{xy} and M_{xx}, M_{yy} and M_{xy} are the basic components of stress resultants and stress couples, M_{xx}^s,M_{yy}^s and M_{xy}^s are additional stress couples associated with the transverse shear effects, Q_{xz} and Q_{yz} are transverse stress-strain resultants and I_i are the inertias. They are defined as

$$\{N_x,N_y,N_{xy}\}=\sum_{n=1}^{3}\int_{h_{n-1}}^{h_n}\{\sigma_x^{(n)},\sigma_y^{(n)},\tau_{xy}^{(n)}\}dz, \tag{3.3a}$$
$$\{M_x,M_y,M_{xy}\}=\sum_{n=1}^{3}\int_{h_{n-1}}^{h_n}z\{\sigma_x^{(n)},\sigma_y^{(n)},\tau_{xy}^{(n)}\}dz, \tag{3.3b}$$
$$\{M_x^s,M_y^s,M_{xy}^s\}=\sum_{n=1}^{3}\int_{h_{n-1}}^{h_n}g\{\sigma_x^{(n)},\sigma_y^{(n)},\tau_{xy}^{(n)}\}dz, \tag{3.3c}$$
$$\{Q_{yz},Q_{xz}\}=\hat{K}\sum_{n=1}^{3}\int_{h_{n-1}}^{h_n}g'\{\tau_{yz}^{(n)},\tau_{xz}^{(n)}\}dz, \tag{3.3d}$$
$$\{I_0,I_1,I_2,I_3,I_4,I_5\}=\sum_{n=1}^{3}\int_{h_{n-1}}^{h_n}\rho_{(n)}\{1,z,g,z^2,zg,g^2\}dz, \tag{3.3e}$$

where $\hat{K}$ is the shear correction factor of FDPT.

Using Eq. (2.11) in Eq. (3.3), the stress resultants, for the present FGM plate, can be

related to the displacements as

$$\begin{Bmatrix} N_x \\ N_y \\ N_{xy} \\ M_x \\ M_y \\ M_{xy} \\ M_x^s \\ M_y^s \\ M_{xy}^s \end{Bmatrix} = \begin{bmatrix} A_1 & A_2 & 0 & B_1 & B_2 & 0 & C_1 & C_2 & 0 \\ & A_1 & 0 & B_2 & B_1 & 0 & C_2 & C_1 & 0 \\ & & A_6 & 0 & 0 & B_6 & 0 & 0 & C_6 \\ & & & D_1 & D_2 & 0 & F_1 & F_2 & 0 \\ & & & & D_1 & 0 & F_2 & F_1 & 0 \\ & & & & & D_6 & 0 & 0 & F_6 \\ & & & & & & G_1 & G_2 & 0 \\ & & & & & & & G_1 & 0 \\ \text{symm.} & & & & & & & & G_6 \end{bmatrix} \begin{Bmatrix} \partial_x u \\ \partial_y v \\ \partial_x v + \partial_y u \\ -\partial_x^2 w \\ -\partial_y^2 w \\ -2\partial_x \partial_y w \\ \partial_x \varphi_x \\ \partial_y \varphi_y \\ \partial_x \varphi_y + \partial_y \varphi_x \end{Bmatrix} + \begin{Bmatrix} N_x^T \\ N_y^T \\ 0 \\ M_x^T \\ M_y^T \\ 0 \\ \bar{M}_x^T \\ \bar{M}_y^T \\ 0 \end{Bmatrix}, \tag{3.4a}$$

$$\begin{Bmatrix} Q_{yz} \\ Q_{xz} \end{Bmatrix} = \begin{bmatrix} H & 0 \\ 0 & H \end{bmatrix} \begin{Bmatrix} \varphi_y \\ \varphi_x \end{Bmatrix}, \tag{3.4b}$$

where

$$\begin{Bmatrix} A_1, & B_1, & C_1, & D_1, & F_1, & G_1 \\ A_2, & B_2, & C_2, & D_2, & F_2, & G_2 \\ A_6, & B_6, & C_6, & D_6, & F_6, & G_6 \end{Bmatrix} = \sum_{n=1}^{3} \int_{h_{n-1}}^{h_n} (1, z, g, z^2, zg, g^2) \begin{Bmatrix} E_1^{(n)} \\ E_2^{(n)} \\ E_3^{(n)} \end{Bmatrix} dz, \tag{3.5a}$$

$$H = \hat{K} \sum_{n=1}^{3} \int_{h_{n-1}}^{h_n} E_3^{(n)} (g')^2 dz, \tag{3.5b}$$

and the thermal force and moment resultants are given by

$$\left\{ N_j^T, M_j^T, \bar{M}_j^T \right\} = \sum_{n=1}^{3} \int_{h_{n-1}}^{h_n} \xi^{(n)}(z) T \left\{ 1, z, g \right\} dz, \quad j = x, y. \tag{3.6}$$

4 Exact solutions for FGM plate

In order to obtain analytical solutions for the dynamic bending problem at hand, Navier's solution is employed here. The determination of transverse deflections and stresses are of fundamental importance in the design of many structural components. The following set of simply supported boundary conditions along the edges of the plate is considered:

$$v = w = \varphi_y = N_x = M_x = M_x^s = T = 0 \qquad \text{at } x = 0, a, \tag{4.1a}$$

$$u = w = \varphi_x = N_y = M_y = M_y^s = T = 0 \qquad \text{at } y = 0, b. \tag{4.1b}$$

Following Navier's solution procedure, we assume the following solution form for $(u, v, w, \varphi_x, \varphi_y)$ that satisfies the simply supported boundary conditions,

$$\left\{ u, \varphi_x \right\} = \left\{ U, \Phi_x \right\} \cos(\lambda x) \sin(\mu y) e^{i\omega t}, \tag{4.2a}$$

$$w = W \sin(\lambda x) \sin(\mu y) e^{i\omega t}, \tag{4.2b}$$

$$\left\{ v, \varphi_y \right\} = \left\{ V, \Phi_y \right\} \sin(\lambda x) \cos(\mu y) e^{i\omega t}, \tag{4.2c}$$

where $\lambda=\pi/a$, $\mu=\pi/b$, $i=\sqrt{-1}$, ω denotes the angular frequency, U, V, W, Φ_x and Φ_y are arbitrary parameters to be determined subjected to the condition that the solution in Eqs. (4.2) satisfies the differential equations (3.2).

The variation of temperature is assumed to occur in the thickness direction according to a power law form. Also, the temperature is supposed to be changed in the plane of the plate as a double Fourier's series in x and y

$$T(x,y,z,t)=\tilde{T}(z)\bar{T}(x,y,t), \tag{4.3}$$

where

$$\tilde{T}(z)=T^b e^{\gamma\left(\frac{z}{h}+\frac{1}{2}\right)^\beta}, \quad \gamma=\ln\left(\frac{T^t}{T^b}\right), \quad 0\leq\beta\leq\infty, \tag{4.4a}$$

$$\bar{T}(x,y,t)=T^*\sin(\lambda x)\sin(\mu y)e^{i\omega t}, \tag{4.4b}$$

in which T^t and T^b are the top and the bottom temperature, β is the temperature exponent and T^* is an arbitrary parameter. Note that $\beta=0$ represents a top surface temperature of the plate while $\beta=\infty$ represents a bottom surface temperature. The assumed temperature function T identically satisfies the boundary conditions (4.1) at the edges of the plate.

Dynamic equilibrium equations can be extended in terms of the parameters U, V, W, Φ_x, Φ_y and T^* by substituting Eq. (3.4a) into Eq. (3.2) with the help of Eqs. (4.2) and (4.3) as

$$\left[L\right]\left\{\Delta\right\}=\left\{F\right\}, \tag{4.5}$$

where

$$\left\{\Delta\right\}=\left\{U \quad V \quad W \quad \Phi_x \quad \Phi_y\right\}^t. \tag{4.6}$$

The superscript "t" represents the transpose of the given vector. The components of the symmetric matrix $[L]$ and the components of the thermal load vector $\{F\}$ are given in Appendix.

5 Numerical results and discussions

Numerical results are presented in this section for perfect, simply supported sandwich plates with FGM faces and homogeneous core resting on two-parameter Pasternak's elastic foundations and subjected to a transient thermal load. The constituent materials of the FGM symmetric and nonsymmetric sandwich plates are taken to be either an aluminum alloy (Al) and silicon carbide (SiC) or an aluminum alloy (Al) and zirconia ZrO_2. Values of parameters for these materials [31] are shown in Table 1.

Table 1: Material properties of aluminum alloy Al, silicon carbide SiC and zirconia ZrO_2 [31].

Properties	Constitutes		
	Al	SiC	ZrO_2
Young's modulus (GPa)	70	427	151
Poisson's ratio	0.3	0.17	0.3
Coefficient of thermal expansion $(10^{-6}/\mathrm{C})$	23.40	4.30	10
Density $(\mathrm{kg/m^3})$	2707	3100	3000

The used non-dimensional parameters are

$$w^*=\frac{10D}{a^4}\mathrm{Re}\Big[w\Big(\frac{a}{2},\frac{b}{2},t\Big)\Big],\qquad \sigma_1=\frac{10^{-3}h^2}{a^2}\mathrm{Re}\Big[\sigma_x\Big(\frac{a}{2},\frac{b}{2},z,t\Big)\Big],$$
$$\sigma_6=\frac{10^{-3}h^2}{a^2}\mathrm{Re}\big[\sigma_{xy}(0,0,z,t)\big],\qquad \sigma_5=\frac{10^(-3)h}{a}\mathrm{Re}\Big[\tau_{xz}\Big(0,\frac{b}{2},z,t\Big)\Big],$$
$$J_1=\frac{K_\mathrm{w}a^4}{D},\quad J_2=\frac{K_\mathrm{p}a^2}{D},\qquad D=\frac{h^3E_\mathrm{c}}{12(1-\nu_\mathrm{c}^2)},\quad T_r=\frac{T^t}{T^b}.$$

The stresses and central deflection of many kinds of Al+SiC/SiC/Al+SiC and Al+ZrO_2/ZrO_2/Al+ZrO_2 sandwich plates are illustrated here by exhibiting several examples using the following fixed data (unless otherwise stated) $a/h=10$, $J_1=J_2=100$, $a=b=0.5\mathrm{m}$, $k=3$, $T^b=20^\circ\mathrm{C}$, $\omega=2\mathrm{s}^{-1}$, $T^*=2$, $T_r=3$, $t=2\mathrm{s}$.

Tables 2-4 display the central deflection $(-w^*)$, in-plane normal stress $(-\sigma_1,\ z=h/2)$ and transverse shear stress $(-\sigma_5,\ z=0)$ for various types of the Al+SiC/SiC/Al+SiC FGM sandwich plates without elastic foundation or resting on Winkler's foundation or Pasternak's foundations for different values of the power law index k using the SDPT, HDPT,

Table 2: The deflection $(-w^*)$ of FGM sandwich plates without or resting on elastic foundations for different values of the power law index k ($\beta=2$, $T_r=2,4$, $t=3\mathrm{sec}$).

Sandwich Type	Theory	$J_1=J_2=0$			$J_1=300,\ J_2=0$			$J_1=300,\ J_2=200$		
		$k=0$	$k=3$	$k=7$	$k=0$	$k=3$	$k=7$	$k=0$	$k=3$	$k=7$
1-1-1	CPT	1.57776	1.71420	1.73544	1.63760	1.78159	1.80427	3.26941	3.69115	3.77420
	FDPT	1.52956	1.71684	1.74778	1.58751	1.78433	1.81709	3.16646	3.69683	3.80092
	HDPT	1.52983	1.71425	1.74246	1.58780	1.78164	1.81157	3.16701	3.69127	3.78943
	SDPT	1.52993	1.71402	1.74204	1.58791	1.78140	1.81113	3.16723	3.69076	3.78850
2-1-2	CPT	1.57775	1.73893	1.76436	1.63759	1.80811	1.83539	3.26940	3.79479	3.90307
	FDPT	1.52955	1.74948	1.78738	1.58750	1.81908	1.85933	3.16642	3.81772	3.95369
	HDPT	1.52983	1.74486	1.77908	1.58780	1.81428	1.85070	3.16701	3.80767	3.93546
	SDPT	1.52994	1.74449	1.77840	1.58791	1.81388	1.84998	3.16727	3.80688	3.93394
2-2-1	CPT	1.57775	-1.25776	-2.17906	1.63759	-1.30690	-2.26482	3.26940	-2.69043	-4.69759
	FDPT	1.52955	-1.25763	-2.19163	1.58750	-1.30678	-2.27788	3.16642	-2.69018	-4.72458
	HDPT	1.52983	-1.25599	-2.18869	1.58780	-1.30508	-2.27481	3.16701	-2.68668	-4.71829
	SDPT	1.52994	-1.25579	-2.18847	1.58791	-1.30487	-2.27459	3.16725	-2.68623	-4.71784
2-1-4	CPT	1.57775	7.13004	13.49832	1.63759	7.41486	14.04318	3.26940	15.63244	29.95441
	FDPT	1.52956	7.20630	13.85310	1.58752	7.49413	14.41212	3.16646	15.79857	30.73187
	HDPT	1.52983	7.19091	13.82542	1.58780	7.47816	14.38334	3.16702	15.76520	30.67204
	SDPT	1.52992	7.19016	13.82745	1.58790	7.47736	14.38546	3.16723	15.76355	30.67661

Table 3: The longitudinal stress $(-\sigma_1)$ in FGM sandwich plates without or resting on elastic foundations for different values of the power law index k ($\beta=2$, $T_r=2$, $t=3$sec).

Sandwich Type	Theory	$J_1=J_2=0$			$J_1=300$, $J_2=0$			$J_1=300$, $J_2=200$		
		$k=0$	$k=3$	$k=7$	$k=0$	$k=3$	$k=7$	$k=0$	$k=3$	$k=7$
1-1-1	CPT	0.71414	1.29276	1.11353	0.71455	1.29280	1.11075	0.72585	1.29537	1.11770
	FDPT	0.70286	1.28883	1.11424	0.70325	1.28892	1.08494	0.71387	1.29153	1.13195
	HDPT	0.70474	1.29040	1.09226	0.70512	1.29040	1.08714	0.71580	1.29292	1.09747
	SDPT	0.70487	1.29041	1.10556	0.70526	1.29051	1.08554	0.71594	1.29289	1.11907
2-1-2	CPT	0.71414	1.06287	0.46387	0.71455	1.06292	0.46352	0.72585	1.06560	0.47607
	FDPT	0.70286	1.05818	0.45668	0.70324	1.05822	0.45609	0.71385	1.06097	0.46043
	HDPT	0.70474	1.06009	0.45685	0.70512	1.06019	0.45796	0.71580	1.06313	0.45767
	SDPT	0.70487	1.06031	0.45968	0.70527	1.06043	0.45558	0.71595	1.06341	0.46842
2-2-1	CPT	0.71413	1.35896	1.11732	0.71455	1.35894	0.98729	0.72585	1.35803	1.33412
	FDPT	0.70285	1.36077	1.08404	0.70323	1.36060	1.01347	0.71384	1.35835	-0.59890
	HDPT	0.70474	1.36064	1.37210	0.70513	1.36078	1.64326	0.71580	1.35998	3.10806
	SDPT	0.70487	1.36031	1.27553	0.70527	1.36050	1.32573	0.71595	1.35768	1.93380
2-1-4	CPT	0.71424	0.89678	-0.40904	0.71464	0.89732	-0.40740	0.72596	0.91224	-0.33962
	FDPT	0.70286	0.86878	-0.49525	0.70334	0.86929	-0.49197	0.71398	0.88439	-0.40926
	HDPT	0.70474	0.87480	-0.50549	0.70513	0.87475	-0.49284	0.71575	0.89020	-0.46428
	SDPT	0.70487	0.87506	-0.48075	0.70524	0.87607	-0.48519	0.71599	0.89092	-0.44228

Table 4: The transverse shear stress $(-\sigma_5)$ in FGM sandwich plates without or resting on elastic foundations for different values of the power law index k ($\beta=2$, $T_r=2$, $t=3$sec).

Sandwich Type	Theory	$J_1=J_2=0$			$J_1=300$, $J_2=0$			$J_1=300$, $J_2=200$		
		$k=0$	$k=3$	$k=7$	$k=0$	$k=3$	$k=7$	$k=0$	$k=3$	$k=7$
1-1-1	FDPT	0.24715	0.45283	0.52018	0.24741	0.45281	0.52011	0.25472	0.45236	0.51791
	HDPT	0.30717	0.40064	0.44091	0.30750	0.40062	0.44086	0.31666	0.40060	0.43928
	SDPT	0.31681	0.40311	0.44051	0.31718	0.40311	0.44048	0.32663	0.40317	0.43894
2-1-2	FDPT	0.24714	0.53462	0.65260	0.24741	0.53457	0.65245	0.25475	0.53267	0.64814
	HDPT	0.30718	0.46494	0.55006	0.30752	0.46490	0.54995	0.31669	0.46357	0.54648
	SDPT	0.31682	0.46549	0.54662	0.31717	0.46546	0.54648	0.32662	0.46422	0.54315
2-2-1	FDPT	0.24714	-0.31086	-0.59834	0.24741	-0.31086	-0.59829	0.25474	-0.31089	-0.59608
	HDPT	0.30718	-0.37174	-0.68266	0.30752	-0.37175	-0.68257	0.31669	-0.37203	-0.68095
	SDPT	0.31682	-0.38576	-0.70589	0.31717	-0.38576	-0.70582	0.32662	-0.38609	-0.70420
2-1-4	FDPT	0.24715	1.70037	2.70869	0.24741	1.70002	2.70758	0.25474	1.68999	2.67488
	HDPT	0.30718	1.77267	2.94380	0.30751	1.77236	2.94269	0.31667	1.76343	2.91042
	SDPT	0.31683	1.81858	3.03596	0.31717	1.81827	3.03483	0.32662	1.80930	3.00197

FDPT, and CPT. It is seen that, the transverse central deflection and the in-plane normal stress have a noticeable increment with the presence of the elastic foundations. Whereas the transverse shear stress have a slight decrement with the presence of the elastic foundations. Also, it can be note that the results increase with the increase of the metal constituents in the plates, whether that is by increasing the thickness of the top and bottom layers or the power law index k. The results of CPT are greater than those of the shear deformation plate theories. The error in the CPT value for the deflection and stresses can be attributed to the large shear deformation that occurs in thick plates. The results predicted by the SDPT are in excellent agreement with those predicted by the HDPT. The disagreement between FDPT and HDPT is much less than the disagreement between any of them and CPT.

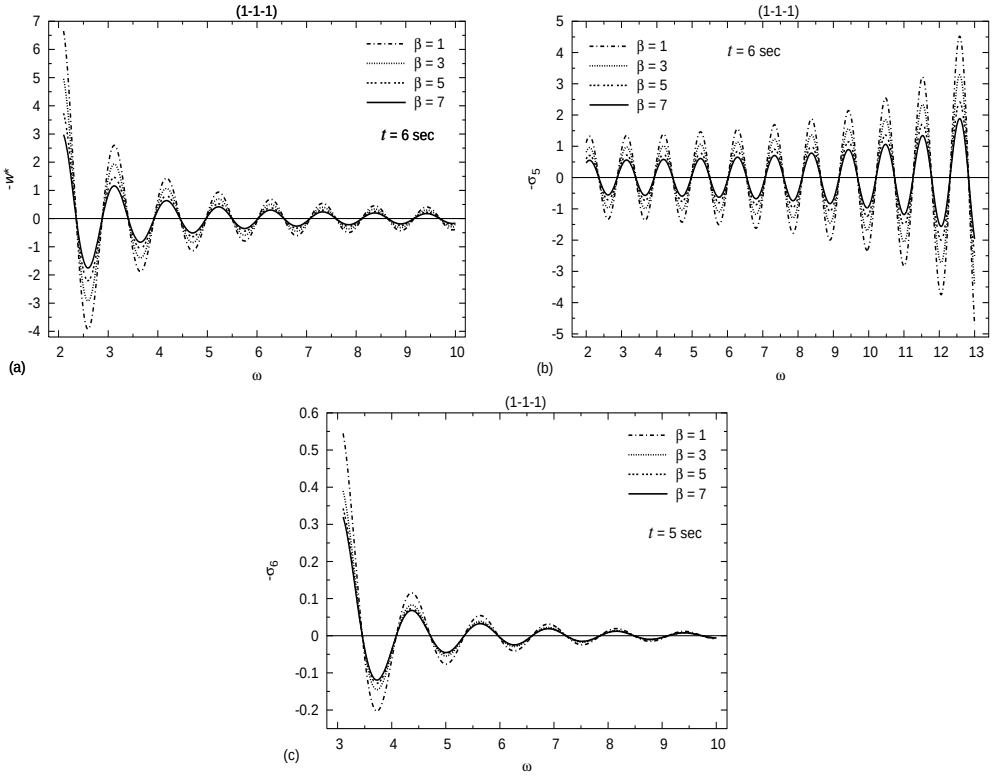

Figure 3: Variation of (a) the deflection $(-w^*)$, (b) the transverse shear stress $(-\sigma_5)$ and (c) the in-plane shear stress $(-\sigma_6)$ in the (1-1-1) FGM plate versus the frequency parameter ω for different values of the temperature exponent β $(T_r=4)$.

Fig. 3 shows plots of the central deflection $(-w^*)$, the transverse shear stress $(-\sigma_5)$ and the in-plane shear stress $(-\sigma_6)$, respectively, of the (1-1-1) Al+SiC/SiC/Al+SiC FGM sandwich plate vs the frequency parameter ω for different values of the temperature exponent β. It is clear that the increase of the temperature exponent β leads to a significant decrement in the variation of the deflection and stresses. The maximum values of the central deflection and the in-plane shear stress decrease gradually as the the frequency parameter ω increases while the change of the maximum of the transverse shear stress is reversed.

The following results are estimated for different types of FGM sandwich plates ($a/h=8$) which are made of aluminum alloy and zirconia. These plates are also resting on elastic foundations and subjected to a time harmonic temperature load. Effect of the power law index k on the deflection w^* and the stresses σ_1 and σ_5 for FGM sandwich plates resting on elastic foundations is explained in Figs. 4-6. It is to be noted that the deflection of the metallic plate is the largest magnitude and that of the ceramic plate is the smallest magnitude. The deflections of the FGM sandwich plates decrease as a/h increases and may be unchanged for $a/h>15$ (see Fig. 4). The FGM sandwich plates with

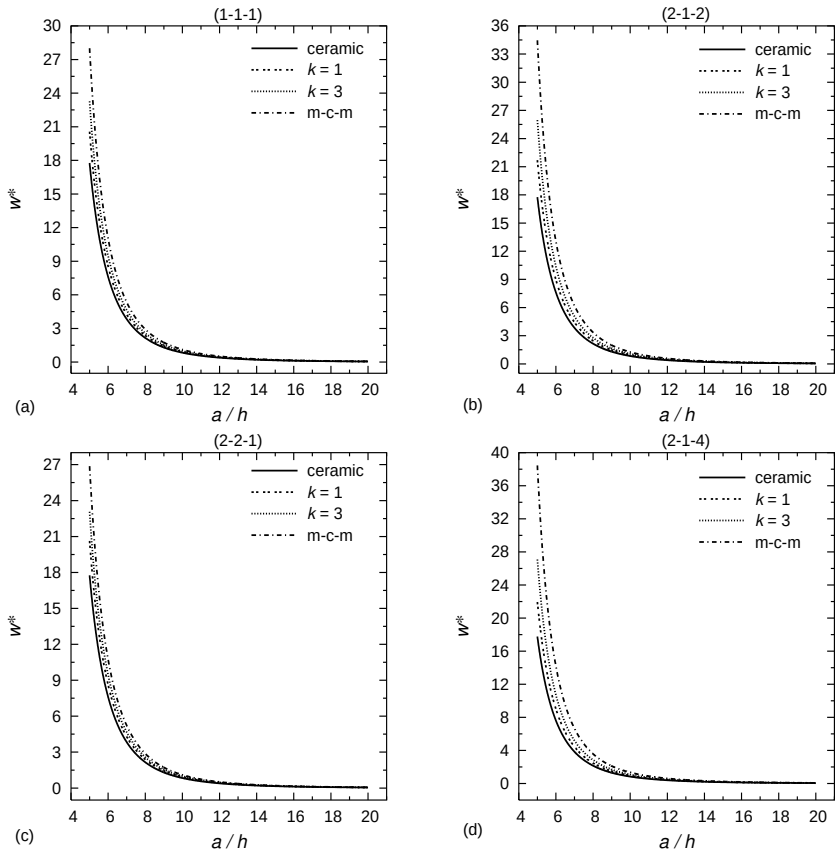

Figure 4: The deflection w^* versus a/h for different values of the power law index k and various types of FGM sandwich plates: (a) The (1-1-1) FGM sandwich plate, (b) The (2-1-2) FGM sandwich plate, (c) The (2-2-1) FGM sandwich plate, (d) The (2-1-4) FGM sandwich plate ($\beta=1$).

intermediate properties undergo corresponding intermediate values of center deflection. This is expected because the metallic plate is the one with the lowest stiffness and the ceramic plate is the one with the highest stiffiness. Figs. 5 and 6 show the variation of σ_1 and σ_5 through-the-thickness of the varied plates for $k=0,1,3,5,\infty$. It is clear that the maximum value of the stress σ_1 in the ceramic plate ($k=0$) occurs at the top surface of the plate, while it occurs at the upper interface in the other types. However, the maximum values of the stress σ_5 in the symmetric sandwich plates, as shown in Figs. 6(a) and (b), occur at the midplane of the plate. The maximums of σ_5 in the symmetric and non-symmetric sandwich plates increase as k increases. Note that, for $k=1$, the stresses σ_1 and σ_5 in the FGM layers vary as linear functions of the thickness coordinate z.

Figs. 7-9 exhibit the variation of the deflection w^* vs the side-to-thickness ratio a/h and the stresses σ_1 and σ_5 through-the-thickness of the (2-1-4) and (2-2-1) FGM sandwich plates for different values of the temperature parameter T^* and the ratio of the top surface temperature to the bottom one $T_r=T^t/T^b$. With the increase of the temperature parameter

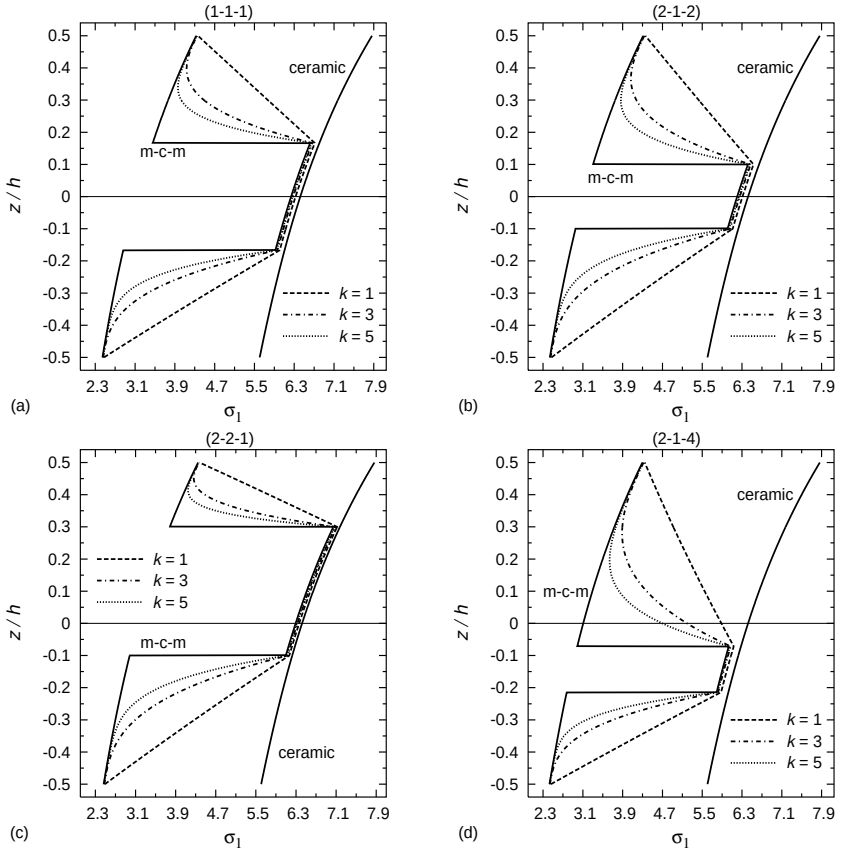

Figure 5: Through-thickness distributions of in-plane normal stress σ_1 for various values of the power law index k and various types of FGM sandwich plates: (a) The (1-1-1) FGM sandwich plate, (b) The (2-1-2) FGM sandwich plate, (c) The (2-2-1) FGM sandwich plate, (d) The (2-1-4) FGM sandwich plate ($\beta=1$).

T^* and the ratio T_r, the deflection w^* and the stresses σ_1 and σ_5 increase.

In order to evaluate the effect of the elastic foundation parameters on the transverse deflection and the stresses of the FGM sandwich plate, we carried out the numerical calculations by varying k_2 for different values of k_1 as investigated in Fig. 10. The deflection and the stresses increase directly separately faraway with an increase in the value of k_2. Also, they increase as Winkler's parameter increases.

6 Conclusions

The dynamic bending of simply supported FGM sandwich plates resting on two-parameter Pasternak's elastic foundations are illustrated by using the SDPT, HDPT and FDPT as well as CPT. Material properties of the sandwich plate faces are assumed to be graded in the thickness direction according to a simple power law distribution in terms

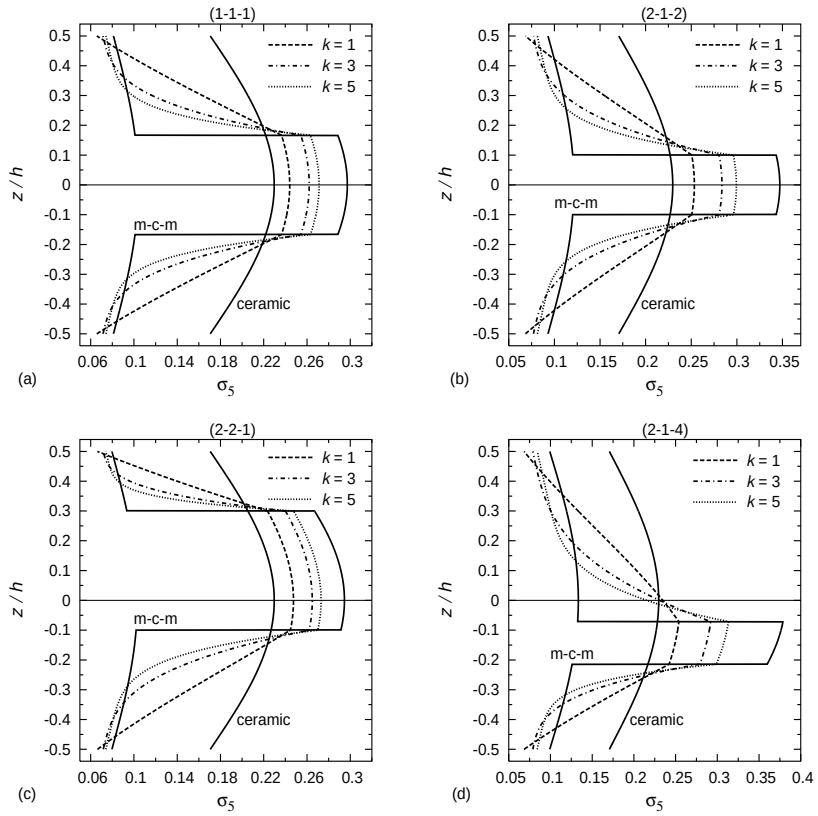

Figure 6: Through-thickness distributions of the transverse shear stress σ_5 for various values of the power law index k and various types of FGM sandwich plates: (a) The (1-1-1) FGM sandwich plate, (b) The (2-1-2) FGM sandwich plate, (c) The (2-2-1) FGM sandwich plate, (d) The (2-1-4) FGM sandwich plate ($\beta=1$).

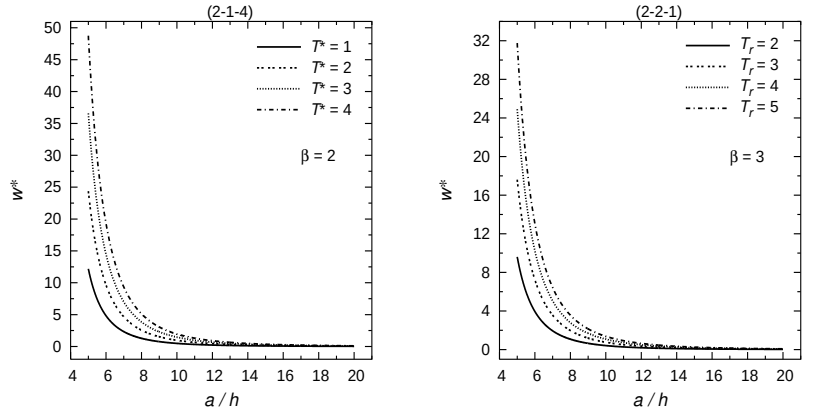

Figure 7: The deflection w^* of the FGM sandwich plates versus the side-to-thickness ratio a/h for different values of the temperature parameter T^* and the top-to-bottom surface temperature ratio T_r.

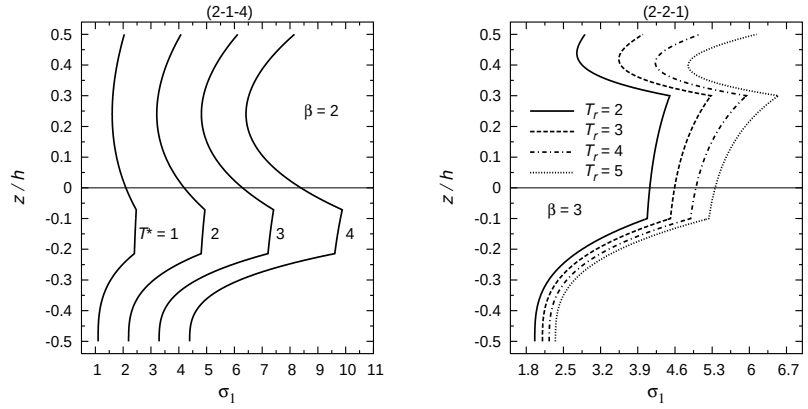

Figure 8: Through-thickness distributions of in-plane normal stress σ_1 in the FGM sandwich plates for different values of the temperature parameter T^* and the top-to-bottom surface temperature ratio T_r.

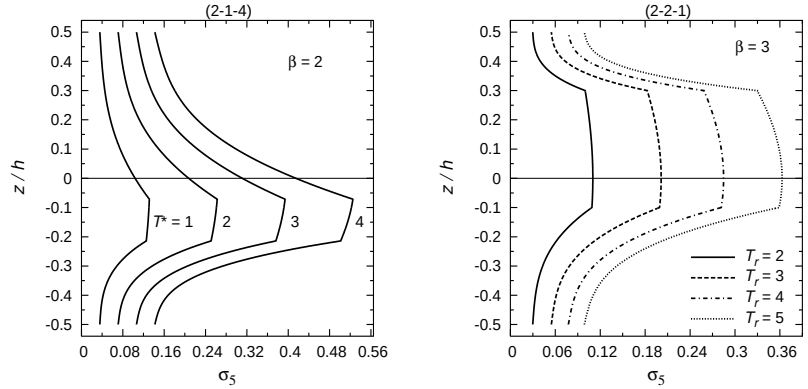

Figure 9: Through-thickness distributions of the transverse shear stress σ_5 in the FGM sandwich plates for different values of the temperature parameter T^* and the top-to-bottom surface temperature ratio T_r.

of the volume fractions of the constituents. The core layer is still homogeneous and made of an isotropic material. Several kinds of symmetric and non-symmetric sandwich plates are studied. Motion equations of FGM sandwich plates including the thermal effects are solved analytically. The numerical results show that the stresses and central deflection are proportional to the temperature parameter T^*, the top-to-bottom surface temperature ratio T_r, Winkler's and shear foundation parameters. The results decrease with the increase of the temperature exponent β and they are very sensitive to the variation of the power law index.

Appendix

The components L_{ij} of the symmetric matrix $[L]$ and the components F_i of the thermal lo-

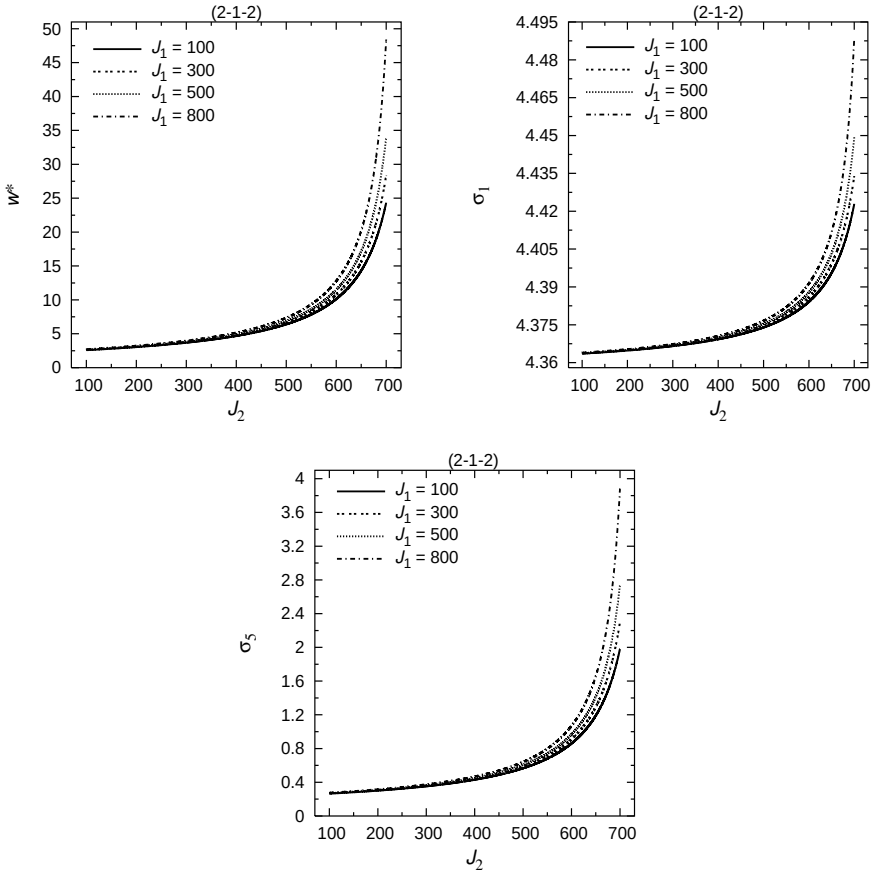

Figure 10: The deflection w^* and the stresses σ_1 and σ_5 of the (2-1-2) FGM sandwich plate versus Pasternak's parameter J_2 for different values of Winkler's parameter J_1 ($\beta=1$).

ad vector $\{F\}$ are given as

$$L_{11}=-A_1\lambda^2-A_6\mu^2+I_0\omega^2, \qquad L_{12}=-(A_2+A_6)\lambda\mu,$$
$$L_{13}=B_1\lambda^3+(B_2+2B_6)\lambda\mu^2-I_1\lambda\omega^2, \qquad L_{14}=-C_1\lambda^2-C_6\mu^2+I_2\omega^2,$$
$$L_{15}=-(C_2+C_6)\lambda\mu, \qquad L_{22}=-A_1\mu^2-A_6\lambda^2+I_0\omega^2,$$
$$L_{23}=B_1\mu^3+(B_2+2B_6)\lambda^2\mu-I_1\mu\omega^2, \qquad L_{24}=L_{15},$$
$$L_{25}=-C_1\mu^2-C_6\lambda^2+I_2\omega^2,$$
$$L_{33}=-D_1(\lambda^4+\mu^4)-2(D_2+2D_6)\lambda^2\mu^2-K_{\rm w}+I_0\omega^2-(K_{\rm p}-I_3\omega^2)(\lambda^2+\mu^2),$$
$$L_{34}=F_1\lambda^3+(F_2+2F_6)\lambda\mu^2-I_4\lambda\omega^2, \qquad L_{35}=F_1\mu^3+(F_2+2F_6)\lambda^2\mu-I_4\mu\omega^2,$$
$$L_{44}=-G_1\lambda^2-G_6\mu^2-H+I_5\omega^2, \qquad L_{45}=-(G_2-G_6)\lambda\mu,$$
$$L_{55}=-G_1\mu^2-G_6\lambda^2-H+I_5\omega^2,$$

and

$$F_1=-T^*A^T\lambda,\quad F_2=-T^*A^T\mu,\quad F_3=T^*B^T(\lambda^2+\mu^2),$$
$$F_4=-T^*C^T\lambda,\quad F_5=-T^*C^T\mu,\quad \left\{A^T,B^T,C^T\right\}=\sum_{n=1}^{3}\int_{h_{n-1}}^{h_n}\xi^{(n)}(z)T^b e^{\gamma\left(\frac{z}{h}+\frac{1}{2}\right)^\beta}\left\{1,z,g\right\}dz.$$

References

[1] A. M. ZENKOUR, *A comprehensive analysis of functionally graded sandwich plates: part 1-deflection and stresses*, Int. J. Solids Struct., 42 (2005), pp. 5224–5242.

[2] A. M. ZENKOUR AND N. A. ALGHAMDI, *Thermomechanical bending response of functionally graded nonsymmetric sandwich plates*, J. Sandwich Struct. Mater., 12 (2010), pp. 7–46.

[3] H. M. SHODJA, H. HAFTBARADARAN AND M. ASGHARI, *A thermoelasticity solution of sandwich structures with functionally graded coating*, Compos. Sci. Technol., 67 (2007), pp. 1073–1080.

[4] J. ZHAO, Y. LI AND X. AI, *Analysis of transient thermal stress in sandwich plate with functionally graded coatings,* Thin Solid Films, 516 (2008), pp. 7581–7587.

[5] T. A. ANDERSON, *A 3D elasticity solution for a sandwich composite with functionally graded core subjected to transverse loading by a rigid sphere*, Compos. Struct., 60 (2003), pp. 265–274.

[6] M. KASHTALYAN AND M. MENSHYKOVA, *Three-dimensional elasticity solution for sandwich panels with a functionally graded core,* Compos. Struct., 87 (2009), pp. 36–43.

[7] J. N. REDDY, *Analysis of functionally graded plates*, Int. J. Numer. Methods Eng., 47 (2000), pp. 663–684.

[8] J. N. REDDY AND Z. Q. CHENG, *Three-dimensional thermomechanical deformations of functionally graded rectangular plates*, Euro. J. Mech. A Solids, 20 (2001), pp. 841–855.

[9] S. S. VEL AND R. C. BATRA, *Three-dimensional analysis of transient thermal stresses in functionally graded plates*, Int. J. Solids Struct., 40 (2003), pp. 7181–7196.

[10] A. M. ZENKOUR, *The refined sinusoidal theory for FGM plates on elastic foundations*, Int. J. Mech. Sci., 51 (2009), pp. 869–880.

[11] A. M. ZENKOUR, *On vibration of functionally graded plates according to a refined trigonometric plate theory*, Int. J. Struct. Stab. Dynam., 5 (2005), pp. 279–297.

[12] A. M. ZENKOUR, *Analytical solutions for rotating exponentially-graded annular disks with various boundary conditions*, Int. J. Struct. Stab. Dynam., 5 (2005), pp. 557–577.

[13] A. M. ZENKOUR, *Steady-state thermoelastic analysis of a functionally graded rotating annular disk*, Int. J. Struct. Stab. Dynam., 6 (2006), pp. 559–574.

[14] A. M. ZENKOUR, *Stresses in a rotating variable-thickness heterogeneous viscoelastic composite cylinder*, Appl. Math. Mech. Engl. Ed., 32(4) (2011), pp. 1–14.

[15] A. M. ZENKOUR, K. A. ELSIBAI AND D. S. MASHAT, *Elastic and viscoelastic solutions to rotating functionally graded hollow and solid cylinders*, Appl. Math. Mech. Engl. Ed., 29 (2008), pp. 1601–1616.

[16] A. M. ZENKOUR AND M. SOBHY, *Elastic foundation analysis of uniformly loaded functionally graded viscoelastic sandwich plates*, J. Mech., 28(3) (2012), pp. 439–452.

[17] A. M. ZENKOUR AND M. SOBHY, *Dynamic bending response of thermoelastic functionally graded plates resting on elastic foundations*, Aerosp. Sci. Technol., 29 (2013), pp. 7–17.

[18] K. MORFIDIS, *Vibration of Timoshenko beams on three-parameter elastic foundation*, Comput. Struct., 88 (2010), pp. 294–308.

[19] E. WINKLER, Die Lehre von der Elastizitat und Festigkeit, Dominicus, Prague, 1867.
[20] B. UĞURLU, A. KUTLU, A. ERGIN AND M. H. OMURTAG, *Dynamics of a rectangular plate resting on an elastic foundation and partially in contact with a quiescent fluid*, J. Sound Vib., 317 (2008), pp. 308–328.
[21] P. L. PASTERNAK, *On a new method of analysis of an elastic foundation by means of two-constants*, Moscow, USSR: Gosudarstvennoe Izdatelstvo Literaturi po Stroitelstvu I Arkhitekture (in Russian).
[22] H. P. LEE, *Dynamic response of a Timoshenko beam on a Winkler foundation subjected to a moving mass*, Appl. Acoust., 55 (1998), pp. 203–215.
[23] K. AL-HOSANI, S. FADHIL AND A. EL-ZAFRANY, *Fundamental solution and boundary element analysis of thick plates on Winkler foundation*, Comput. Struct., 70 (1999), pp. 325–336.
[24] K. M. LIEW, J.-B HAN, Z. M. XIAO AND H. DU, *Differential quadrature method for Mindlin plates on Winkler foundations*, Int. J. Mech. Sci., 38 (1996), pp. 405–421.
[25] J.-B. HAN AND K. M. LIEW, *Numerical differential quadrature method for Reissner/Mindlin plates on two-parameter foundations*, Int. J. Mech. Sci., 39 (1997), pp. 977–989.
[26] H.-S. SHEN AND L. YU, *Nonlinear bending behavior of Reissner-Mindlin plates with free edges resting on tensionless elastic foundations*, Int. J. Solids Struct., 41 (2004), pp. 4809–4825.
[27] Z. Y. HUANG, C. F. LÜ AND W. Q. CHEN, *Benchmark solutions for functionally graded thick plates resting on Winkler-Pasternak elastic foundations*, Compos. Struct., 85 (2008), pp. 95–104.
[28] A. M. ZENKOUR, M. N. M. ALLAM AND M. SOBHY, *Bending analysis of FG visco-elastic sandwich beams with elastic cores resting on Pasternak's elastic foundations*, Acta Mech., 212 (2010), pp. 233–252.
[29] A. M. ZENKOUR, M. N. M. ALLAM AND M. SOBHY, *Bending of a fiber-reinforced viscoelastic composite plate resting on elastic foundations*, Arch. Appl. Mech., 81 (2011), pp. 77–96.
[30] G. V. PRAVEEN AND J. N. REDDY, *Nonlinear transient thermoelastic analysis of functionally graded ceramic-metal plates*, Int. J. Solids Struct., 35 (1998), pp. 4457–4476.
[31] Y. Y. LEE, X. ZHAO AND K. M. LIEW, *Thermoelastic analysis of functionally graded plates using the element-free kp-Ritz method*, Smart Mater. Struct., 18 (2009), pp. 1–15.
[32] N. NODA AND B. L. WANG, *Transient thermoelastic responses of functionally graded materials containing collinear cracks*, Eng. Fract. Mech., 69 (2002), pp. 1791–1809.
[33] S. S. VEL AND R. C. BATRA, *Exact solution for thermoelastic deformations of functionally graded thick rectangular plates*, AIAA J., 40 (2002), pp. 1421–1433.
[34] A. M. ZENKOUR AND M. SOBHY, *Thermal buckling of various types of FGM sandwich plates*, Compos. Struct., 93 (2010), pp. 93–102.
[35] A. M. ZENKOUR AND M. SOBHY, *Thermal buckling of functionally graded plates resting on elastic foundations using the trigonometric theory*, J. Thermal Stresses, 34 (2011), pp. 1119–1138.
[36] H.-S SHEN, *Nonlinear bending response of functionally graded plates subjected to transverse loads and in thermal environments*, Int. J. Mech. Sci., 44 (2002), pp. 561–584.
[37] P. H. WEN, M. H. ALIABADI AND A. YOUNG, *A boundary element method for dynamic plate bending problems*, Int. J. Solids Struct., 37 (2000), pp. 5177–5188.
[38] X. WANG, Y. X. WANG AND H. K. YANG, *Dynamic interlaminar stresses in laminated plates with simply and fixed supports*, subjected to Free Vib. Thermal Load. Compos. Struct., 68 (2005), pp. 139–145.
[39] L. GUO AND J. YU, *Dynamic bending response of double cylindrical tubes filled with aluminum foam*, Int. J. Impact Eng., 38 (2011), pp. 85–94.